

Article

# A Comprehensive Study of a New 1.75 Hydrate of Ciprofloxacin Salicylate: SCXRD Structure Determination, Solid Characterization, Water Stability, Solubility, and Dissolution Study

Ilma Nugrahani <sup>1,\*</sup> , Billgerd Tjengal <sup>1,\*</sup>, Tutus Gusdinar <sup>1</sup>, Ayano Horikawa <sup>2</sup> and Hidehiro Uekusa <sup>2</sup> 

<sup>1</sup> Department of Pharmacochemistry, School of Pharmacy, Bandung Institute of Technology, Bandung 40132, Indonesia; gusdinar@fa.itb.ac.id

<sup>2</sup> Department of Chemistry, Tokyo Institute of Technology, Tokyo 152-8551, Japan; a.horikawa.chem@gmail.com (A.H.); uekusa@chem.titech.ac.jp (H.U.)

\* Correspondence: ilma\_nugrahani@fa.itb.ac.id (I.N.); billgerd.tjengal@gmail.com (B.T.)

Received: 7 March 2020; Accepted: 17 April 2020; Published: 28 April 2020



**Abstract:** One problem that often arises during the formulation of a dosage form is the solubility and dissolution of the active ingredients. This problem arises in ciprofloxacin, which is a BCS class IV fluoroquinolone antibiotic. A pseudopolymorph is a kind of polymorph in which the number of hydrates is different. In this study, a new pseudopolymorph comprised of ciprofloxacin and salicylic acid was found, namely the salt ciprofloxacin salicylate 1.75 hydrate form. This new solid phase was analyzed by Fourier-transform infrared spectroscopy (FTIR), Raman spectroscopy, and thermal analysis and proven by Powder X-ray Diffractometry (PXRD) analysis. The crystal structure was successfully determined by Single Crystal X-ray Diffractometry (SCXRD) analysis. It was found that the piperazinyl group of ciprofloxacin is protonated by H<sup>+</sup> from the carboxylic group of salicylic acid. In the unit cell, two ciprofloxacin and two salicylic acid molecules were independent with four water molecules, in which one water molecule had 0.5 occupancy due to inversion symmetry. Interestingly, this hydrate crystal dehydrated by grinding for 105 minutes forms an anhydrous crystalline phase, which was analyzed with FTIR, Raman spectroscopy, thermal analysis, and PXRD. The solubility and dissolution tests were carried out using UV-Visible spectrophotometry and a multiple linear regression method. This new hydrate solid phase has a better profile than the original ciprofloxacin crystal, according to the solubility and dissolution tests.

**Keywords:** ciprofloxacin; salicylic acid; pseudopolymorph; solubility enhancing; dissolution enhancing; dehydration; milling; Raman spectroscopy; multilinear regression

## 1. Introduction

Fluoroquinolones are one of the most widely used synthetic antibiotics nowadays and they are the first line therapy for the infection of Gram-negative bacteria, such as *Pseudomonas aeruginosa* [1]. Antibiotics in this group work by inhibiting enzymes that are involved in DNA replication: DNA topoisomerase IV and DNA gyrase [2]. The mechanism of action is specific to bacteria, due to the difference in DNA replication enzymes that are present in bacteria and mammals. Ciprofloxacin is one of the most popular fluoroquinolones and it is taken via the oral route. The drug is mostly marketed in the form of solid dosage forms, especially tablets.

The problem that arises when formulating an oral drug is its solubility and permeability. These two parameters will decide whether an orally administered drug will generate high systemic

bioavailability [3–5]. Ciprofloxacin is classified as a BCS (Biopharmaceutical Classification System) class IV compound, meaning that it possesses poor solubility as well as poor gastrointestinal permeability [6]. Co-crystal and salt formation are two popular approaches for improving the bioavailability of oral drugs by modifying the solubility profile [7].

In the market, ciprofloxacin is sold in the form of a salt with hydrochloric acid (ciprofloxacin HCl). The main problem with this approach is that the HCl in the active pharmaceutical might interact with the acid found in the stomach via a common ion effect, thereby potentially decreasing the solubility and consequent bioavailability [8]. One method for counteracting this issue is to form an organic salt of ciprofloxacin instead of using hydrochloric acid. One counter-ion of choice is the hydroxybenzoic anion, including salicylic acid.

When an acid and a base containing a hydrogen-bonding donor and acceptor group are mixed, two possible products may be formed: salt or co-crystal [9]. In the salt, the constituents interact via ionic bonds, while the interaction in the co-crystal is in the form of hydrogen bonds [10]. The probability of generating each product varies, depending on the difference between the  $pK_a$  values of the acid and the base. According to Cruz-Cabeza, when the  $pK_a$  difference is greater than 3, salt is expected to form [11]. Salicylic acid has a  $pK_a$  of 2.97, whilst the piperazinyl ring of ciprofloxacin has a  $pK_a$  of 8.74. Ciprofloxacin should be able to form a salt with salicylic acid, according to the previously mentioned rule.

During the course of this research, two papers have been published that had also found multicomponent crystals of ciprofloxacin and salicylic acid [12,13]. However, the salt that was obtained from this research had a different crystalline structure to those of the previously published papers.

## 2. Materials and Methods

### 2.1. Chemicals

Ciprofloxacin HCl (Merck, Berlin, Germany), salicylic acid (Merck, Berlin, Germany), methanol (Sigma Aldrich, Darmstadt, Germany), ethanol (Sigma Aldrich, Darmstadt, Germany), KBr Fourier-transform infrared spectroscope (FTIR) grade (Merck, Tokyo, Japan), sodium hydroxide (Merck, Berlin, Germany), sodium dihydrogen phosphate (Sigma Aldrich, Darmstadt, Germany), and distilled water was prepared by School of Pharmacy, Bandung Institute of Technology.

### 2.2. Instruments

Ultrasonicator (Wiseclean WUC-D06H, Gangwon-do, South Korea), pH meter (Mettler Toledo, Columbus, California, USA), melting point analyzer (Electrothermal IA9000, Staffordshire, UK), optical microscope (Yazumi XSZ-107BN 1600X, Jakarta, Indonesia), Fourier-transform infrared spectroscope (FTIR) (Jasco FT/IR-4200 type A, Easton, Pennsylvania, USA), Raman spectrometer (Bruker-Senterra, Billerica, Massachusetts USA), powder X-ray diffractometer (Bruker D8 Advance, Billerica, Massachusetts, USA), single crystal X-ray diffractometer (Rigaku R-AXIS RAPID, Tokyo, Japan), thermogravimetric analysis/differential thermal analysis (TG/DTA) (Hitachi STA7300, Hitachi, Japan), type 2 dissolution apparatus (Guoming RC-1, Tianjin Guoming Medicinal Equipment, Tianjin, China), orbital shaker (Hinotek KJ-210 BD, Ningbo, China), and UV-Visible spectrophotometer (HP/Agilent 8453, Santa Clara, California, USA).

### 2.3. Methods

#### 2.3.1. Multicomponent Salt Formation

##### Ciprofloxacin Base Preparation

One gram of ciprofloxacin HCl was dissolved in 50 mL of distilled water. NaOH 0.1 N was added drop-wise to the solution until the pH reached  $7.42 \pm 0.5$ . The resulting precipitates were filtered while using a vacuum pump and then dried.

## Binary Phase Diagram Construction

A series of physical mixtures consisting of ciprofloxacin base and salicylic acid in stoichiometric ratios of (1:9), (1:4), (1:3), (1:2), (2:3), (3:4), (5:5), (4:3), (3:2), (2:1), (3:1), (4:1), and (9:1) were prepared. The melting point of each mixture was determined using a melting point analyzer with a temperature range from 100–400 °C and a heating rate of 10 °C/min.

## Ciprofloxacin Salicylate 1.75 Hydrate Salt Formation

Equimolar amounts of ciprofloxacin and salicylic acid were dissolved in a methanol-water (1:1) mixture. The solution was sonicated for 20 min. at room temperature. The crystals were grown by the slow evaporation of the solvent in a fume hood. The resulting crystal was stored inside an opaque and dark container inside a desiccator.

### 2.3.2. Characterization

#### Fourier-Transform Infrared Spectroscopy (FTIR)

The samples were mixed with KBr and compressed into clear pellets. The spectra were recorded in the wavenumber range between 4000 and 400  $\text{cm}^{-1}$  at a resolution of 4  $\text{cm}^{-1}$ .

#### Raman Spectroscopy

Samples were placed in the holder. The spectra were recorded using an Nd:YAG 785 nm DPSS (Diode-Pumped Solid-State) laser with a power of 25 mW for 10 sec. Each spectrum was read at a Raman shift of 59–2626  $\text{cm}^{-1}$ .

#### Powder X-ray Diffractometry (PXRD)

The reflectant Powder X-ray Diffractometry (PXRD) was performed using a Bruker D8 Advance (Billerica, Massachusetts, USA) and then illuminated with the radiation of Cu-K $\alpha$  ( $\lambda = 1.5418 \text{ \AA}$ ) at a tube voltage of 40 kV and a tube current of 35 mA. The samples were analyzed over a  $2\theta$  range of 25–45° with a scanning rate of 4°/min.

#### Single Crystal X-ray Diffractometry (SCXRD)

The samples were analyzed by the Rigaku R-Axis RAPID with the radiation of Cu-K $\alpha$  ( $\lambda = 1.5418 \text{ \AA}$ ) while using a graphite monochromator at 173 K. The integrated and scaled data were empirically corrected for the absorption effects using ABSCOR. The structure was solved using a dual space algorithm that was implemented in SHELXT and then refined on F2 using SHELXL-2017/1. All of the non-hydrogen atoms were anisotropically refined. The hydrogen atoms attached to nitrogen and oxygen atoms, except for water oxygen, were located using the differential Fourier map, but treated using a riding model at the geometrically calculated position during the refinement. The water hydrogen atoms were isotropically refined with the standard bond distance restraints. Other hydrogen atoms were geometrically determined and they were included in the calculation using the riding model. The molecular graphics were produced using Mercury 4.3.1 [14] and Chem3D 15.1.

#### Thermal Analysis

The samples were placed in an aluminum pan and then heated at a temperature range between 30 °C and 350 °C with a heating rate of 10 °C/min. An empty aluminum pan was used as a reference. All of the pans were closed during the analysis.

### 2.3.3. Performance Evaluation

#### Solubility Study

The solubility study was conducted in HCl pH 1.2 and phosphate buffer pH 6.8 media. The samples were weighed and placed inside the media following agitation using an orbital shaker. The concentration of ciprofloxacin in the solution was determined every 24 hours using a UV-Visible spectrophotometer. More samples were added when the solution appeared to be clear (the samples were completely dissolved). The study was terminated when the addition of sample did not affect the concentration of the solution. The result was compared to the physical mixture and ciprofloxacin alone.

#### Dissolution Study

The dissolution study was conducted at 37 °C in HCl pH 1.2 and phosphate buffer pH 6.8 medium. The medium was stirred at 50 rpm. The salts were weighed to be equivalent to 500 mg of ciprofloxacin. One mL of the sample was taken at 5, 10, 15, 30, 45, 60, 90, and 120 min. The concentration of ciprofloxacin was determined while using a UV-Visible spectrophotometer. The results were compared to the physical mixture and ciprofloxacin alone.

### 2.3.4. Dehydration

The ciprofloxacin salicylate 1.75 hydrate salt crystals were ground in a mortar for 105 minutes by hand. The crystals were then analyzed using Raman spectroscopy, TG/DTA, and PXRD.

## 3. Results

### 3.1. Multicomponent Salt Formation

Because the basic form of ciprofloxacin is not widely available on the market nowadays, the salt must be converted into its basic form. The ciprofloxacin base was prepared by treating ciprofloxacin HCl solution with a strong base (NaOH) in low molarity until the pH reached  $7.42 \pm 0.5$ . At this pH, the ionic interaction that was previously formed between the N atom in the piperazinyl moiety of ciprofloxacin with the chloride ion in HCl disappeared due to the formation of a zwitterion [15]. This species possesses low solubility in aqueous solution due to the net charge value of zero. Therefore, precipitation occurred, and ciprofloxacin could be obtained by simple filtration. The yield of ciprofloxacin obtained from this method was around 69.47%.

### 3.2. Binary Phase Diagram Construction

In this research, an attempt was made to produce multicomponent crystals that consist of a ciprofloxacin base and salicylic acid. The physical interaction between two substances can be predicted by constructing a binary phase diagram. In theory, different products are possibly generated when two molecules physically interact. Based on the pKa of the starting materials, a co-crystal or salt will be formed by two constituents when the binary phase diagram shows a letter "W" profile [16–20], indicating a certain stoichiometric ratio with a higher melting point between two eutectic or peritectic points. The binary phase diagram showed either a congruent or incongruent melting point. The binary phase diagram between ciprofloxacin and salicylic acid revealed that either the co-crystal or the salt may be formed when an equimolar amount (1:1) of each component was mixed, as shown in Figure 1. This equimolar ratio was then used for the production of salt.

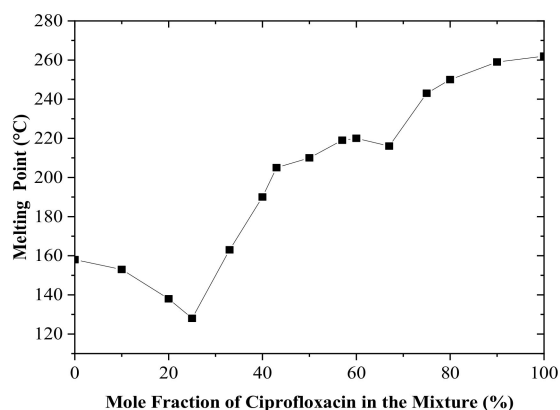


**Figure 1.** Binary phase diagram of a ciprofloxacin and salicylic acid mixture.

### 3.3. Ciprofloxacin Salicylate 1.75 Hydrate Crystal Preparation

The multicomponent crystal consisting of ciprofloxacin and salicylic acid was obtained from the solvent evaporation method while using methanol-water (1:1). The slow evaporation method is a popular method for generating crystals with adequate size for SCXRD analysis [21]. The solvent should be able to dissolve both the drug and the counter-ion, thus enabling the interaction between components. The solvent polarity should be carefully considered to achieve this condition, mainly when a co-solvent is used [22]. Ciprofloxacin and salicylic acid can be considered as slightly nonpolar substances, with Log P values of 0.28 and 2.26, respectively [23,24]. Therefore, the use of an organic solvent is necessary. Methanol was chosen due to its availability and low vapor pressure, thus it easily evaporates. Figure 2 shows the macroscopic and microscopic morphology of the resulting crystals that were obtained from the slow evaporation method. The crystal is brittle and it exhibits a clear to off-white needle shape with a length of 5 mm.

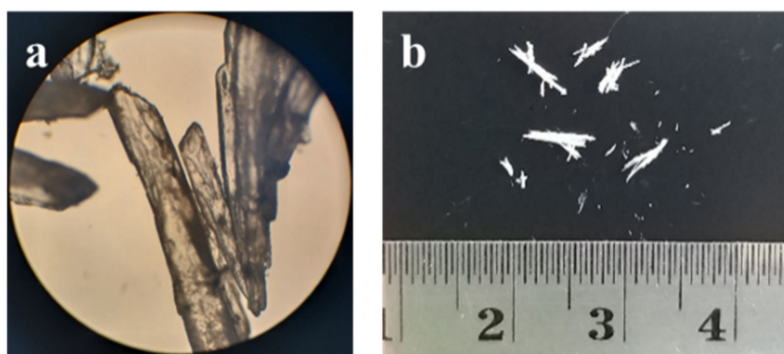


**Figure 2.** Morphological observation of ciprofloxacin salicylate crystals (a) under a microscope with 10x magnification and (b) without a visualizing aid.

### 3.4. Characterization

#### 3.4.1. Fourier-Transform Infrared Spectroscopy (FTIR)

Infrared spectroscopy enables the observation of intramolecular and intermolecular bonds [25]. Thus, the instrument is regularly involved in crystal engineering and material science. The piperazinyl ring in the ciprofloxacin and carboxylic group in salicylic acid have pKa values of 8.74 and 2.97, respectively [23,24]. According to the “rule of three” [5], the difference between these pKa values (i.e. 5.77) indicates the formation of salt when the two constituents were mixed [20]. Ciprofloxacin will act as a base and it undergoes protonation in the piperazinyl moiety. In accordance with this hypothesis, a band at a wavelength of  $2492\text{ cm}^{-1}$ , which corresponds to the N-H stretch of positively charged N-atoms in the piperazinium group, is observed in both ciprofloxacin HCl and ciprofloxacin

salicylate (Figure 3). The band is absent in the ciprofloxacin FTIR spectrum. This finding suggested that ciprofloxacin and salicylic acid formed a salt, with ionic interactions between the positively charged N-atom in the piperazinium moiety of ciprofloxacin and negatively-charged carboxylic moiety in salicylic acid. However, this result does not necessarily confirm the absence of intermolecular hydrogen bonds. X-ray diffractometry can be used to accurately determine the crystalline structure [26,27].

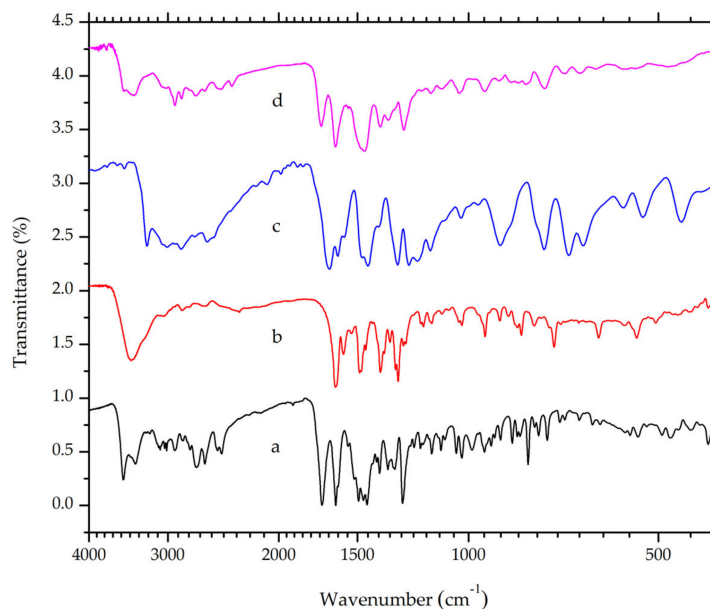


**Figure 3.** Overlaid Fourier-Transform Infrared Spectroscopy (FTIR) spectra of (a) ciprofloxacin HCl, (b) ciprofloxacin base, (c) salicylic acid and (d) a ciprofloxacin salicylate multicomponent crystal.

A strong band at around  $1700\text{ cm}^{-1}$  was observed in ciprofloxacin as well as its salt due to the asymmetric stretching of the C=O bond in the carboxylic acid group [28]. However, this band will shift to a shorter wavelength range when the carboxylic group is deprotonated. Ciprofloxacin exhibited a peak at around  $1579\text{ cm}^{-1}$ , which corresponds to the asymmetric vibration of O-C-O, as shown in Figure 3 [29]. Meanwhile, salicylic acid exhibited distinctive peaks at  $3236$  and around  $3008\text{--}2858\text{ cm}^{-1}$ , which indicate O-H and C-H stretch, respectively. Symmetric and asymmetric C=O stretch was observed at a wavelength of  $1662$  and  $1388\text{ cm}^{-1}$ . At the range  $760\text{--}660\text{ cm}^{-1}$ , peaks that indicate =C-H bending in a benzene ring were also observed [30]. The multicomponent crystal of ciprofloxacin salicylate showed no overlapping peaks when overlaid on the FTIR spectra of ciprofloxacin and salicylic acid. This result indicates that the multicomponent salt was successfully obtained with no residue of its starting materials.

#### 3.4.2. Raman Spectroscopy

Raman spectroscopy is another form of vibrational spectroscopy, which has also been used in crystal engineering as a complement for FTIR. In Figure 4, a peak at Raman shift value of  $1384\text{ cm}^{-1}$  was observed in ciprofloxacin and its salt due to the stretching vibration of the quinolone ring. The peak is still present in ciprofloxacin salicylate multicomponent crystal [31] with slight differences. Distinctive peaks of the salt crystal were shown at Raman shift values of  $1627$ ,  $1540$ , and  $1390$ , which correspond to C=O stretching in the quinolone moiety, anti-symmetric O-C-O, and symmetric O-C-O of the carboxylic acid group. This result supported FTIR spectroscopy, suggesting that the crystal that was obtained from the solvent evaporation method is a salt of ciprofloxacin salicylate.

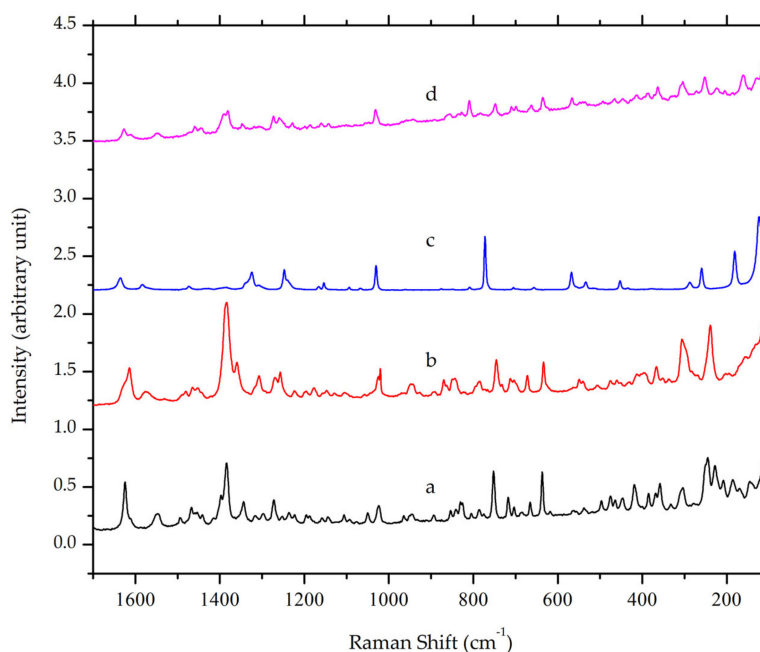


**Figure 4.** Overlaid Raman spectra of (a) ciprofloxacin HCl, (b) ciprofloxacin base, (c) salicylic acid and (d) ciprofloxacin salicylate multicomponent crystal.

### 3.4.3. Powder X-ray Diffractometry (PXRD)

Diffractometry is widely used in crystal engineering and is sometimes used for crystal structure determination [26,27,32–35]. Powder diffractometry is more convenient to apply when the analyzed solid sample exists in the form of powder. In this research, PXRD was utilized as an initial characterization of the new phase formation. Figure 5a,b revealed the calculated diffractograms of ciprofloxacin base with the CCDC deposition number of 757817 reported by Mahapatra et al., 2010 [36] and salicylic acid CCDC deposition number of 1423858, as published by Woinska et al., 2016 [37], as the starting materials, respectively. Meanwhile, Figure 5c,d are the calculated and the measured diffractograms of ciprofloxacin salicylate 1.75 hydrate (this work; see Section 3.4.4). The measured and calculated diffractograms of the salt hydrate crystal have a similar profile with the strong major intensity peaks observed at  $2\theta = 3.60, 6.69, 7.13, 0.93,$  and  $15.61^\circ$ , as shown in this figure. However, several foreign peaks still existed, which represented a small number of ciprofloxacin and salicylic acid.

Figure 5 also shows that, although the peak positions were almost the same in the measured and calculated diffractograms, the intensities revealed considerable differences. For example, the highest peak of the calculated diffractogram was  $3.60^\circ$ , but it was  $7.13^\circ$  in the measured one. Besides, some parts were enhanced or vanished from the measured one. The preferred orientation effect would cause these conditions due to a specific crystal habit of the small crystals.

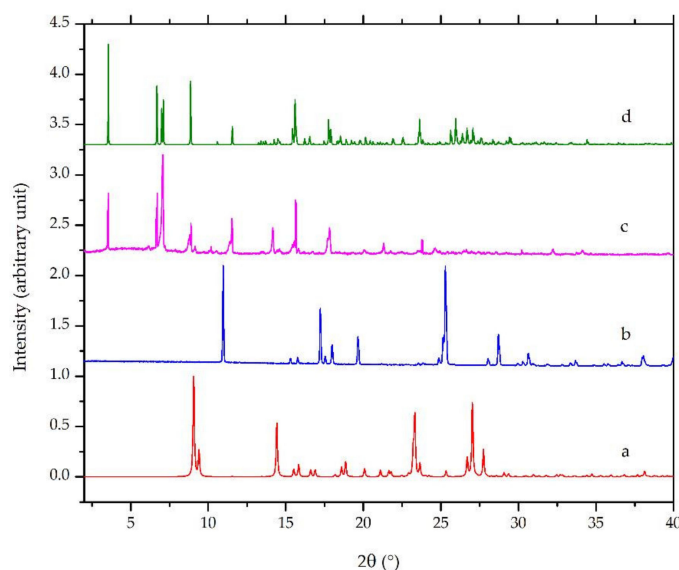


**Figure 5.** Powder X-ray diffractograms of: (a) calculated ciprofloxacin base [36], (b) calculated salicylic acid [37], (c) measured ciprofloxacin salicylate • 1.75 H<sub>2</sub>O, and (d) calculated ciprofloxacin salicylate • 1.75 H<sub>2</sub>O (this work).

#### 3.4.4. Single Crystal X-ray Diffractometry (SCXRD)

Aside from PXRD, SCXRD is also widely used in crystal engineering for structure determination purposes. In this research, this method determined the crystal structure of ciprofloxacin salicylate salt. The crystallographic data were shown in Table 1. In the asymmetric unit, there were two units of ciprofloxacin salicylate salt and four water molecules (Figure 6). One water molecule (O15) existed near an inversion center, and the intermolecular distance between O15 and O15' [1-x, 1-y, 1-z] was 2.125 Å, which was too short as hydrogen bonded water molecules (standard distance is ca. 2.7 Å, and shortest ca. 2.4 Å). Therefore, the occupancy factor of this water molecule should be 0.5 by this crystallographic symmetry constraint. Thus, the number of water molecules is 3.5 and the formal hydration number of one salt unit is 1.75. The further refinement of this water molecule (O15) occupancy revealed that ca. 55% of it escaped from the specimen single crystal. This occupancy might mean that the water molecule was easily removed from the crystal. We might see the reason in comparison to the number of a hydrogen bond that stabilizes water molecules in the crystal. Only this water molecule had two hydrogen bonds, but the other three water molecules had three bonds. Thus, the actual hydration number would be 1.61. This estimation could explain the TG/DTA result which is described in the Thermal Analysis section. In this report, we used the formal hydration number of 1.75 to present the structure.

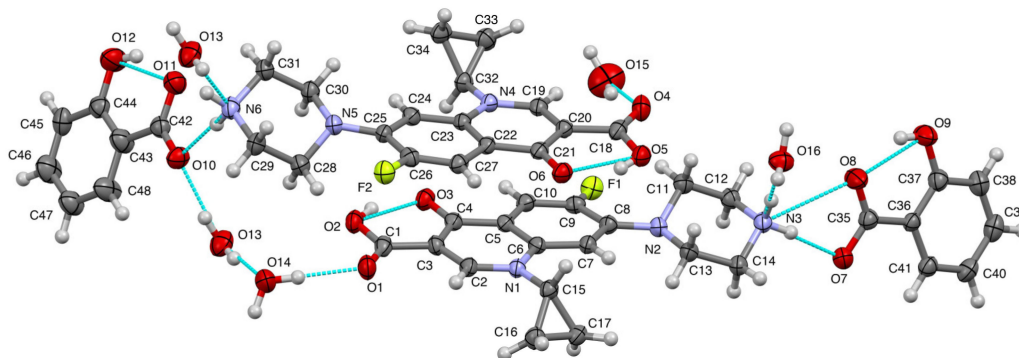
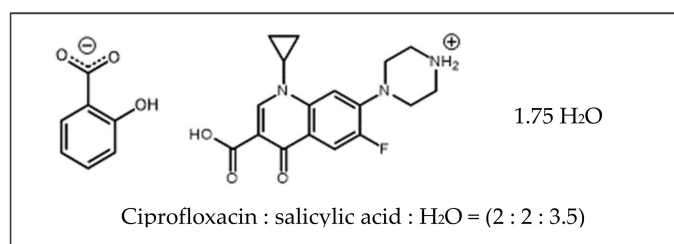


**Figure 6.** The molecular drawing of ciprofloxacin salicylate • 1.75 H<sub>2</sub>O with 30% probability thermal ellipsoids. Blue broken lines show the hydrogen bonds.

**Table 1.** Crystal data ciprofloxacin salicylate • 1.75 H<sub>2</sub>O.

Formula	(C <sub>17</sub> H <sub>19</sub> FN <sub>3</sub> O <sub>3</sub> ) <sub>2</sub> (C <sub>7</sub> H <sub>5</sub> O <sub>3</sub> ) <sub>2</sub> (H <sub>2</sub> O) <sub>3.5</sub>
Crystal System	Monoclinic
Space group	<i>P</i> 2 <sub>1</sub> / <i>n</i>
<i>a</i> /Å	13.4283(3)
<i>b</i> /Å	7.01490(10)
<i>c</i> /Å	49.9625(9)
β/°	95.1830(10)
V/Å <sup>3</sup>	4687.13(15)
Z	4
R <sub>1</sub> /%	8.49



One of the purposes of this crystal structure analysis was to confirm the salt state of these compounds. Based on the pK<sub>a</sub> rule, the piperazinyl ring of ciprofloxacin (pK<sub>a</sub>: 8.74) and COOH of salicylic acid (pK<sub>a</sub>: 2.97) should form a salt. H<sup>+</sup> transferred from COOH of salicylic acid to N of piperazinyl ring of ciprofloxacin. Two apparent residual electron densities (N3: 0.58 and 0.37 eÅ<sup>-3</sup>; N6: 0.43 and 0.32 eÅ<sup>-3</sup>) existed in the chemically expected positions in the piperazinyl N. Additionally, the H atom of COOH of salicylic acid was not found in the residual electron density map to show the deprotonation. From the molecular geometry point of view, the lengths of four C–O of the carboxylic moieties were almost the same (in the range from 1.264(6) to 1.287(6) Å), and the distances between two adjacent C–O lengths were small; these were 0.012 and 0.021 Å.

On the other hand, the COOH groups of ciprofloxacin molecules showed more significant C–O differences that were 0.101 and 0.105 Å, which indicated that COOH structure interacted together with the C=O and C–OH bond. These structural data strongly confirmed that ciprofloxacin–salicylic acid formed a salt. The intramolecular hydrogen bonds were observed in ciprofloxacin and salicylic acid molecule as OH...O<sup>−</sup>, which can be regarded as the charge assisted hydrogen bond, as shown in Figure 6. These hydrogen bonds made a flat molecular conformation from the quinolone of the ciprofloxacin molecule with the carboxylic moiety of salicylic acid. The piperazinium ring exhibited a chair conformation, and NH<sub>2</sub><sup>+</sup> of it had two hydrogen bonds to the water molecule and carboxylate of the salicylic acid molecule (another charge assisted interaction). COOH of ciprofloxacin molecule and a water molecule were connected by the OH...O type hydrogen bond. This type of hydrogen bond was also formed between the water molecules.

Figure 7 shows crystal packing drawing. Ciprofloxacin molecules (blue and green) were stacked with each other (distance was 3.3 to 3.4 Å) due to the π–π interaction between aromatic rings. This new crystal phase has been submitted to Cambridge Crystallographic Data Centre with the deposit number 1983477 with the more detail data can be accessed in Supplementary Material 1.

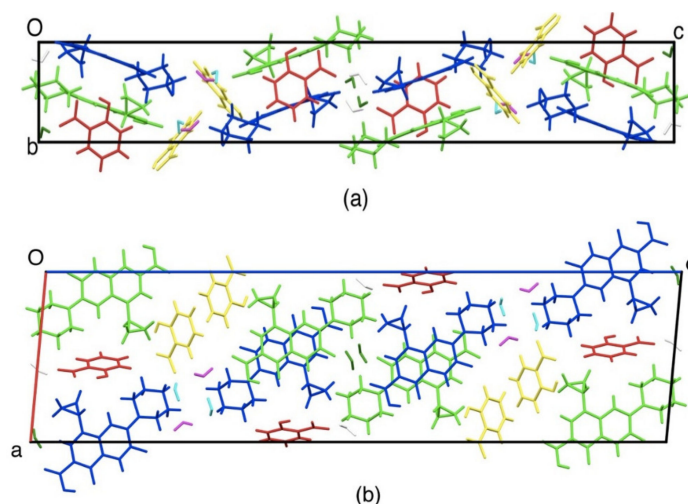


**Figure 7.** Crystal structure of ciprofloxacin salicylate • 1.75 H<sub>2</sub>O salt viewed along. (a) *a*-axis, (b) *b*-axis. Ciprofloxacin: blue and green, salicylate: red and orange.

### 3.4.5. Thermal Analysis

Thermal analysis, such as differential thermal analysis (DTA) combined with thermogravimetric analysis (TG), can be used to determine the melting point, crystallization temperature, heat of crystallization, and decomposition temperature [38]. In this research, DTA/TG was used for thermal analysis. The DTA profile of ciprofloxacin salicylate salt exhibited two endothermic peaks, at a range between 55–65 °C and 215–225 °C, as shown in Figure 8. The first peak indicated the thermal dehydration of the salt crystal lattice [39,40]; the escaping water molecule contributed to the reduction of mass of ca. 5%. The expected mass reduction was 6.3% for the 1.75 hydrate, so the less than expected reduction would correspond to a partial loss of water analyzed by SCXRD, which indicated the 1.61 hydrate phase. In such case, the expected reduction is 5.8%. As for the complete loss of one partial water (O15), 1.5 hydrate phase should show 5.4% reduction. Thus, the mass reduction in TG/DTA measurement also agreed with the occupancy of the partial water. Meanwhile, the second peak indicates the salt melting point. Beyond the melting point, the thermogravimetric analysis showed a steep decline in salt mass, which suggested that the sample decomposed. Ciprofloxacin undergoes decomposition when thermally heated at temperatures above 220 °C [41].

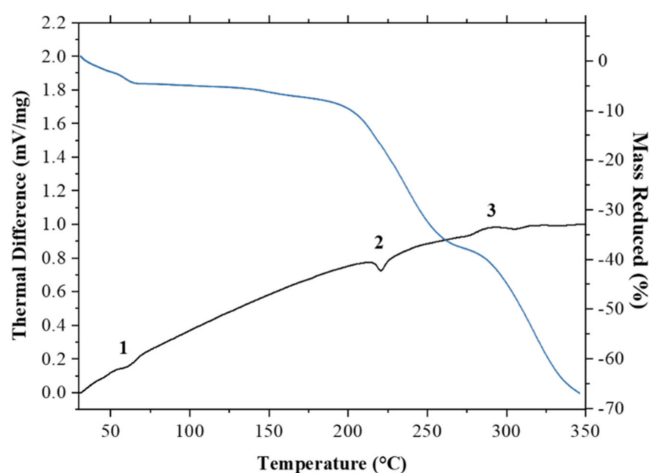


**Figure 8.** Thermograms of ciprofloxacin salicylate • 1.75 H<sub>2</sub>O salt during differential thermal analysis/thermogravimetric analysis (DTA/TG) analysis showing two endothermic peaks indicating (1) the liberation of water molecule and (2) melting point as well as (3) an exothermic peak indicating decomposition.

### 3.5. Performance Evaluation

The main reason behind the co-crystal and salt formation of active pharmaceutical ingredients is to improve its physicochemical properties, especially the solubility and dissolution rate [13,42,43]. The determination of ciprofloxacin content in aqueous medium should be conducted while using an adequate quantitative analytical method. Currently, UV-Visible spectrophotometry and high-performance liquid chromatography (HPLC) are the most popular methods for ciprofloxacin determination [44,45]. In this research, ciprofloxacin content was determined using UV-Visible spectrophotometry in the presence of salicylic acid.

In aqueous solution, ciprofloxacin usually exhibits maximum absorbance at around 278 nm. At this wavelength, salicylic acid was found to interfere with the UV absorbance of ciprofloxacin. Therefore, the direct determination of ciprofloxacin concentration in the presence of salicylic acid will lead to inaccurate results. Furthermore, the UV absorbance spectrum of ciprofloxacin and salicylic acid is affected by pH, due to the difference in the protonation states [46–49], as depicted in Figure 9a,b.

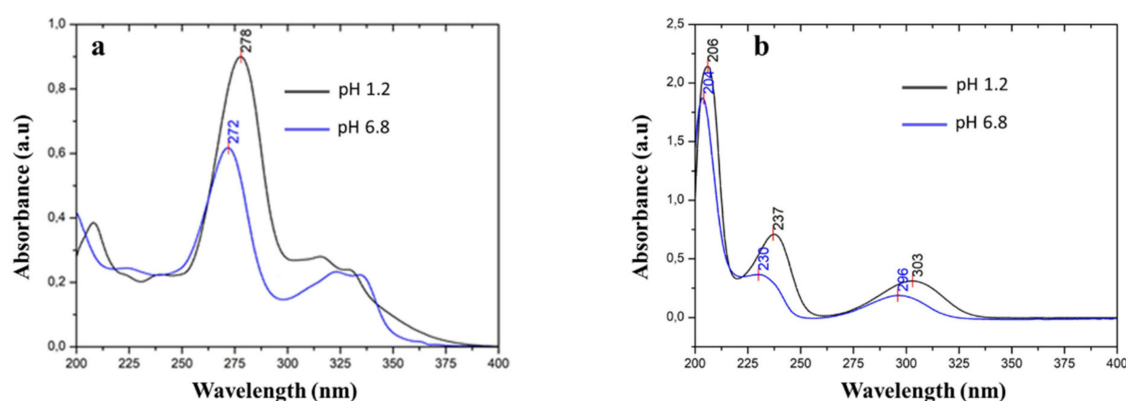


Figure 9. UV spectra of (a) ciprofloxacin and (b) salicylic acid in pH 1.2 and pH 6.8 media.

Ciprofloxacin exhibits maximum absorbance at a wavelength of 278 nm and pH 1.2. This peak shifted to 272 nm at pH 6.8. Meanwhile, salicylic acid exhibits a maximum absorbance at wavelengths of 303, 237, and 206 nm in pH 1.2. The peaks shifted to 296, 230, and 204 nm in pH 6.8. The observable hypsochromic shift for ciprofloxacin at the higher pH was caused by the deprotonation of both carboxylic and piperazinium moieties [48]. In salicylic acid, the shift happened due to the deprotonation of the carboxylic moiety [49].

A simultaneous determination method was used to address the previously mentioned issues. The content determination method can be applied in a multicomponent analysis by constructing a linear equation involving the concentration of both components as independent variables (i.e., multiple linear regression) [50]. In this method, a series of concentrations of ciprofloxacin and salicylic acid mixtures were used to construct a calibration plane. In this study, a series of ciprofloxacin and salicylic acid (Table 2) mixtures were prepared and then measured using a UV-Visible spectrophotometer.

Table 2. Solution series to construct calibration plane.

HCl Buffer pH 1.2		Phosphate Buffer pH 6.8	
Ciprofloxacin (ppm)	Salicylic Acid (ppm)	Ciprofloxacin (ppm)	Salicylic Acid (ppm)
8	0.5	0.5	8
6	4	1	6
5	1.5	2	4
4	2	4	2
3	3	6	1
2	1	8	0.5

The sample was scanned at wavelengths between 200 and 400 nm. The absorbance at each wavelength was plotted against concentration. For pH 1.2, the criterion was met at a wavelength of 278 nm in the zero-order spectrum and at 287 nm for the first-order derivative spectrum. At pH 6.8, the measurement was conducted at 272 nm in a zero-order spectrum; meanwhile, 281 nm in a first-order derivative spectrum. Table 3 shows the resulting simultaneous equations; these equations were used to calculate ciprofloxacin concentration.

**Table 3.** Calibration result of ciprofloxacin and salicylic acid mixture in pH 1.2 and 6.8 media.

Medium	Equation	R <sup>2</sup>
pH 1.2	$A_{278} = -0.0772 + 0.0997 C_{\text{ciprofloxacin}} + 0.0115 C_{\text{salicylic}}$	R <sup>2</sup> = 0.999
pH 1.2	$(dA/d\lambda)_{287} = -0.0003 - 0.0056 C_{\text{ciprofloxacin}} + 0.0016 C_{\text{salicylic}}$	R <sup>2</sup> = 0.999
pH 6.8	$A_{272} = -0.0459 + 0.0891 C_{\text{ciprofloxacin}} + 0.0093 C_{\text{salicylic}}$	R <sup>2</sup> = 0.999
pH 6.8	$(dA/d\lambda)_{281} = 0.0013 - 0.0053 C_{\text{ciprofloxacin}} + 0.0008 C_{\text{salicylic}}$	R <sup>2</sup> = 0.999

### 3.5.1. Solubility Study

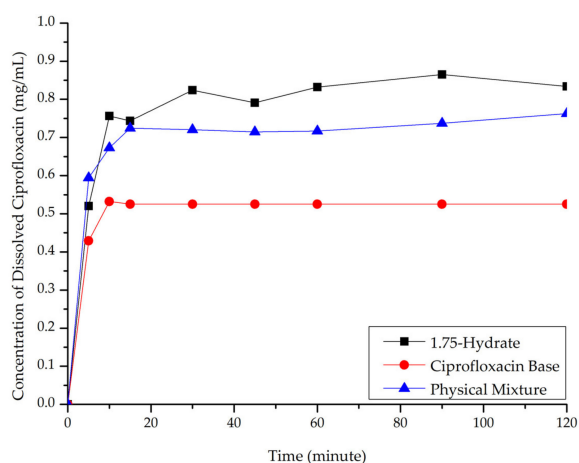
In this study, solubility was evaluated in two media: acidic (pH 1.2) to represent stomach conditions and neutral (pH 6.8) to represent the intestines. Table 4 summarizes the results. The solubility of ciprofloxacin in pH 2.0 and pH 6.8 media is  $7.88 \pm 0.005$  mg/mL and  $0.080 \pm 0.05$  mg/mL, respectively [51]. Assuming that the difference in solubility at pH 2.0 and pH 1.2 is insignificant, ciprofloxacin salicylate salt formation was shown to increase the solubility of ciprofloxacin by 1.3-fold at pH 1.2 and 2.1-fold at pH 6.8.

**Table 4.** Solubility study result of ciprofloxacin salicylate • 1.75 H<sub>2</sub>O salt when compared to the solubility of previously published polymorphs.

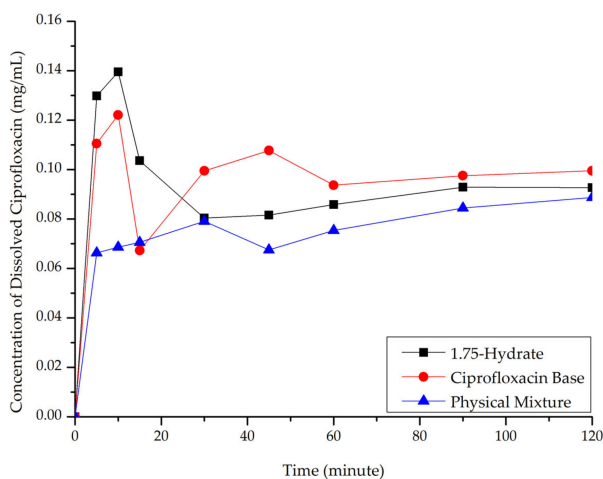
Medium	Sample	Solubility (mg/mL)	Factor of Multiplication
pH 1.2	ciprofloxacin salicylate • 1.75 H <sub>2</sub> O	$10.7 \pm 0.8$	0.96
	ciprofloxacin salicylate • H <sub>2</sub> O polymorph I [13]	$8.8 \pm 0.6$	1.18
	ciprofloxacin salicylate • H <sub>2</sub> O polymorph II [13]	$7.09 \pm 0.02$	1.46
pH 6.8	ciprofloxacin salicylate • 1.75 H <sub>2</sub> O	$1.30 \pm 0.18$	0.13
	ciprofloxacin salicylate • H <sub>2</sub> O polymorph I [13]	$1.10 \pm 0.13$	0.16
	ciprofloxacin salicylate • H <sub>2</sub> O polymorph II [13]	$0.67 \pm 0.04$	0.26

### 3.5.2. Dissolution Study

Ciprofloxacin salicylate 1.75 hydrate salt dissolved more rapidly and reached a higher concentration at a steady-state in pH 1.2 when compared to ciprofloxacin and the physical mixture, as shown in Figure 10a. At pH 6.8 (Figure 10b), although the salt exhibited a higher concentration in the early observation period, the amount of dissolved ciprofloxacin then decreased. This phenomenon was caused by the transformation of ciprofloxacin from the 1.75 salt hydrate to its base form, which is less soluble than the multicomponent crystal [50]. Eventually, the steady-state was reached. The concentration of ciprofloxacin at a steady-state is similar to that of ciprofloxacin alone, physical mixture, and salt. To confirm this phenomenon, PXRD was used to analyze the undissolved material in pH 1.2 media. The result is attached in Supplementary Material 2, which shows the diffractogram consisting of the peaks of starting materials (ciprofloxacin monohydrate and salicylic acid) and the 1.75 salt hydrate. It means that the bond between the two components broke up in this dissolution media and showed the parachute effect, which showed decreasing dissolution after a maximum peak [52].



(a)



(b)

**Figure 10.** Dissolution profile comparison of ciprofloxacin salt, ciprofloxacin and physical mixture in. (a) pH 1.2 and (b) pH 6.8.

### 3.6. Dehydration by Milling

The presence of solvent inside a crystal lattice might affect the physicochemical properties of a drug [53,54]. Savjani et al. [3] reported that most anhydrous crystals have a higher solubility and a faster dissolution rate than their hydrated counterparts. Therefore, in this study, an attempt was made to obtain an anhydrous ciprofloxacin-salicylic salt. In this experiment, the milling represented one of the treatments in the pharmaceutical manufacturing process. In some steps, such as reducing the particle size, mixing, and granulation steps, milling is common to be performed. The effect of milling on the release of the hydrates of amoxicillin trihydrate as well as of fluoroquinolone antibiotics, included ciprofloxacin hydrochloride monohydrate evaluated using FTIR, have been reported [55]. The treatment using milling also can prevent the instability of the main component towards heating [56,57]. A simple mechanochemical method with manual grinding was developed to liberate the water from the crystal lattice [58].

After milling for 105 minutes, the ciprofloxacin salicylate salt crystal was evaluated using FTIR, Raman spectroscopy, DTA/TG, and PXRD. The resulting Raman spectrum (Figure 11) is blue-shifted in the Raman spectrum region of 1500–1600  $\text{cm}^{-1}$ , whilst three peaks are red-shifted in the 150, 350, and 850  $\text{cm}^{-1}$  regions; also, the area under the curve of the -O-H stretching region in the FTIR spectrum (Figure 12) is significantly reduced. These results indicated that the water molecule was successfully

removed from the crystal lattice during the grinding process. This phenomenon is similar to the previous report of ciprofloxacin hydrochloride monohydrate, which released its hydrate's peak after milling [55]. Supplementary Material 3 reveals that PXRD analysis proved that the sample did not interact with KBr during the sample preparation.

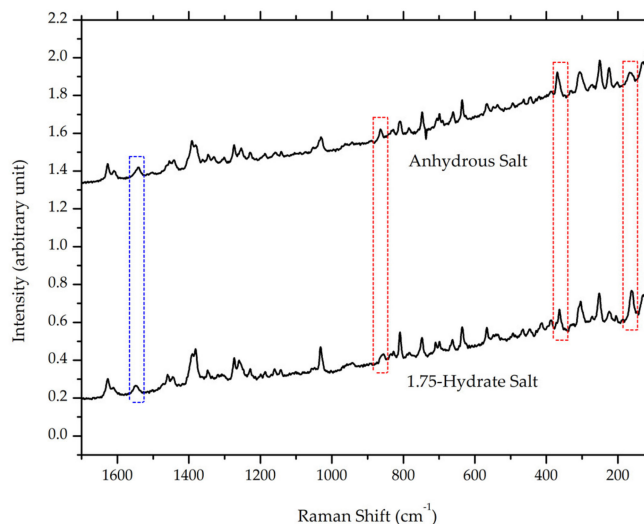


**Figure 11.** Comparison of Raman spectra between ciprofloxacin salicylate • 1.75 H<sub>2</sub>O and anhydrous ciprofloxacin salicylate, red and blue boxes mark red and blue shifts in the spectra, respectively.

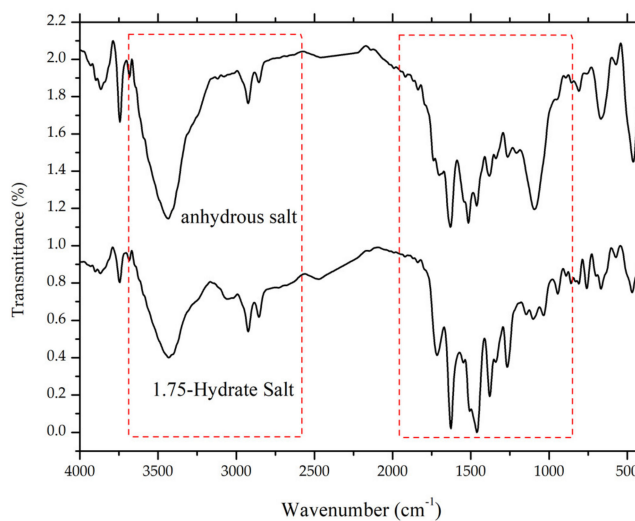
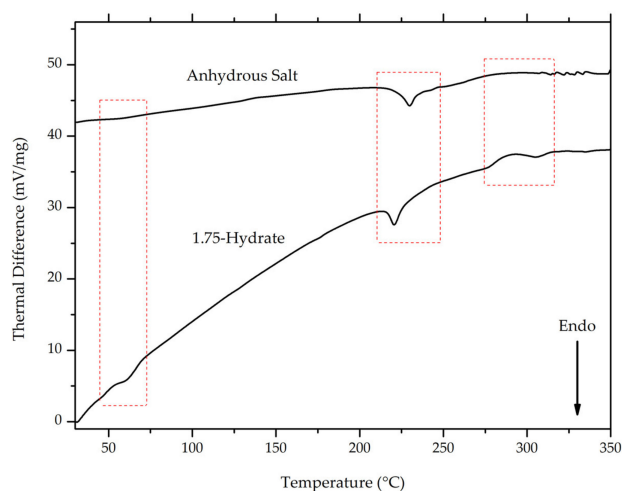
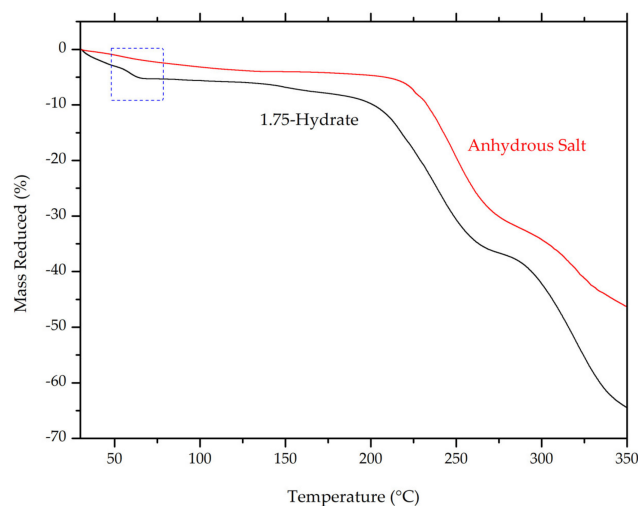


**Figure 12.** Comparison of FTIR spectra between ciprofloxacin salicylate • 1.75 H<sub>2</sub>O and anhydrous ciprofloxacin salicylate, red boxes marks -O-H stretching region.

On the thermal analysis thermogram (Figure 13a,b), the first endothermic peak, which was observed in ciprofloxacin salicylate • 1.75 H<sub>2</sub>O crystal (around 55–65 °C), disappeared. This result confirms the removal of water molecules, since this endothermic peak was previously associated with water evaporation from crystal lattice. The melting point of the salt was slightly shifted to a higher temperature range.



(a)



(b)

**Figure 13.** Comparison of thermogram between ciprofloxacin salicylate • 1.75 H<sub>2</sub>O and anhydrous ciprofloxacin salicylate using (a) DTA and (b) TG, blue boxes indicate the region where changes occur.

Figure 14 compares the diffractogram of the milled sample to the origin phase. Some new peaks appeared after the milling for dehydration process, as shown at  $2\theta = 8, 16.5, 18, 21, 23.5, 26.5,$  and  $27.5^\circ$  (blue markers). However, the small peaks of the original phase still existed, which revealed at  $2\theta = 7$  and  $8.5$  (yellow markers). Besides, a peak at  $2\theta = 12^\circ$  was unsolved yet as a new peak or due to the 1.75 hydrate salt; hence, it is double marked by blue and yellow. The diffractogram of the milled sample shows that a small portion of it might be the milling time is not enough to complete dehydration. These data are in line with the thermogram in Figure 13b, which also indicated a small amount of water appearance in the anhydrous (milled) solid-state curve. Next, the diffractogram of the milled sample's diffractogram was also compared to the anhydrate phase reported by Surov et al., 2019, which was produced from a mechanochemical method using acetonitrile and ethanol. The small peaks at  $2\theta = 6, 9,$  and  $16^\circ$  (red markers) appeared to be similar to the Surov's anhydrous phase of ciprofloxacin salicylate [13]. These data indicate that the measured sample might consist of three phases, namely a new anhydrous phase, the Surov's anhydrous, and a small portion of the 1.75 hydrate form of ciprofloxacin salicylate. Nevertheless, the single crystal of the new polymorph of anhydrous phase cannot be isolated yet; then, it will not be discussed further.

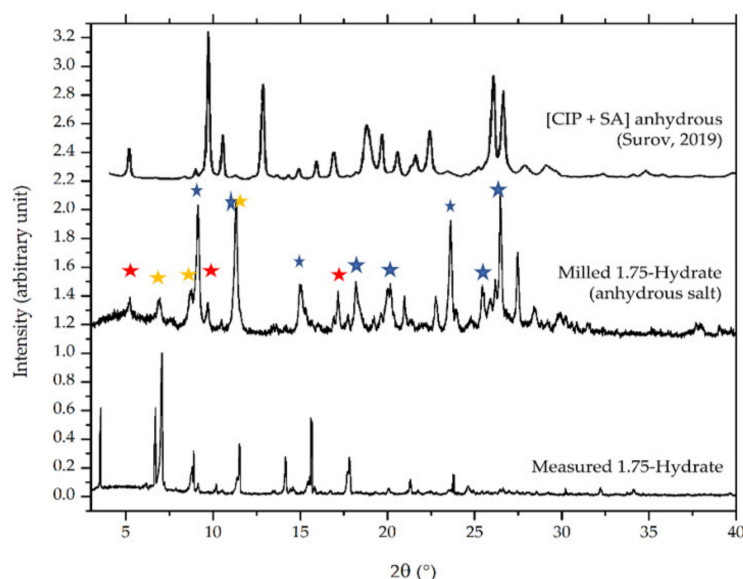


**Figure 14.** Comparison of powder diffractograms between ciprofloxacin salicylate • 1.75 H<sub>2</sub>O, the milled sample, and Surov's anhydrous phase [13]. The red marks indicate Surov's anhydrous peaks; yellow ones are the peaks of origin ciprofloxacin salicylate • 1.75 H<sub>2</sub>O, and the blue ones represent the peaks of a new anhydrous phase yielded after milling.

#### 4. Conclusions

New pseudopolymorph of ciprofloxacin salicylate 1.75 H<sub>2</sub>O that is the salt hydrate between ciprofloxacin and salicylic acid has been discovered and fully characterized by FTIR, Raman spectroscopy, thermal analysis, and PXRD analysis. Additionally, the crystal structure was determined by SCXRD. This multicomponent salt exhibits higher solubility and superior dissolution profile when compared to ciprofloxacin crystal. A simple dehydration process using manual grinding was developed in order to liberate water molecules from the crystal lattice successfully and obtain a new anhydrous phase, which was characterized by Raman spectroscopy, FTIR, thermal analysis, and PXRD analysis.

**Supplementary Materials:** The following are available online at <http://www.mdpi.com/2073-4352/10/5/349/s1>. Parameters of ciprofloxacin salicylate • 1.75 H<sub>2</sub>O crystal; S2. PXRD of ciprofloxacin salicylate • 1.75 H<sub>2</sub>O crystal with KBr; S3. Undissolved material of the hydrate salt's diffractogram.

**Author Contributions:** Conceptualization, I.N., T.G., and B.T.; methodology, I.N., B.T., T.G., A.H., and H.U.; software, B.T., A.H., and H.U.; validation, I.N., B.T., A.H., and H.U.; formal analysis, B.T., A.H.; investigation, B.T. and A.H.; resources, I.N., T.G., and H.U.; data curation, B.T., I.N., H.U.; writing—original draft preparation, I.N., T.G., and B.T.; writing—review and editing, I.N., B.T., T.G., H.U.; visualization, I.N., B.T., A.H., H.U.; supervision, I.N., T.G., and H.U.; project administration, I.N.; funding acquisition, I.N. and H.U. All authors have read and agreed to the published version of the manuscript.

**Funding:** This research was funded by Research and Community Service of Bandung Institute of Technology, Bandung, Indonesia under The Overseas Collaboration Research, World Class University Program, 2020, 018/WCU-ITB/LL/2020. Part of this work was supported by JSPS KAKENHI Grant Number JP17K05745 and JP18H04504 (HU).

**Acknowledgments:** Some parts of the experiments were supported by Uekusa research group, Department of Chemistry, Tokyo Institute of Technology, Japan, and the Physical Chemistry of Material Laboratory, Department of Chemistry, Faculty of Mathematics and Natural Sciences, Bandung Institute of Technology, Indonesia.

**Conflicts of Interest:** The authors declare no conflicts of interest.

## References

1. Troughton, J.A.; Millar, G.; Smyth, E.T.M.; Doherty, L.; McMullan, R. Ciprofloxacin use and susceptibility of Gram-negative organisms to quinolone and non-quinolone antibiotics. *J. Antimicrob. Chemother.* **2011**, *66*, 2152–2158. [[CrossRef](#)] [[PubMed](#)]
2. Aldred, K.J.; Kerns, R.J.; Osherooff, N. Mechanism of quinolone action and resistance. *Biochemistry* **2014**, *53*, 1565–1574. [[CrossRef](#)] [[PubMed](#)]
3. Savjani, K.T.; Gajjar, A.K.; Savjani, J.K. Drug solubility: Importance and enhancement techniques. *ISRN Pharm.* **2012**, 195727. [[CrossRef](#)] [[PubMed](#)]
4. Lu, J.X.; Murray, J. *Biochemistry, Dissolution and Solubility*. StatPearls Publishing: Treasure Island, Florida, 2019. Available online: <https://www.ncbi.nlm.nih.gov/pubmed/28613752> (accessed on 20 November 2019).
5. Khadka, P.; Roa, J.; Kim, H.; Kim, I.; Kim, J.T.; Kim, H.; Cho, J.M.; Yun, G.; Lee, J. Pharmaceutical particle technologies: An approach to improve drug solubility, dissolution and bioavailability. *Asian J. Pharm. Sci.* **2019**, *9*, 304–316. [[CrossRef](#)]
6. Olivera, M.E.; Manzo, R.H.; Junginger, H.E.; Midha, K.K.; Shah, V.P.; Stavchansky, S.; Dressman, J.B.; Barends, D.M. Biowaiver monographs for immediate release solid oral dosage forms: Ciprofloxacin hydrochloride. *J. Pharm. Sci.* **2011**, *100*, 22–33. [[CrossRef](#)]
7. Cavanagh, K.L.; Maheshwari, C.; Hornedo, N.R. Understanding the Differences between Cocrystal and Salt Aqueous Solubilities. *J. Pharm. Sci.* **2018**, *107*, 113–120. [[CrossRef](#)]
8. Bannigan, P.; Verma, V.; Hudson, S.P. Overcoming the Common Ion Effect for Weakly Basic Drugs: Inhibiting the Crystallization of Clofazimine Hydrochloride in Simulated Gastrointestinal Media. *Cryst. Growth Des.* **2019**, *19*, 1599–1609. [[CrossRef](#)]
9. Golovnev, N.N.; Molokey, M.S.; Lesnikov, M.K.; Atuchin, V.V. Two salts and the salt cocrystal of ciprofloxacin with thiobarbituric and barbituric acids: The structure and properties. *J. Phys. Org. Chem.* **2017**, *31*, 1–10. [[CrossRef](#)]
10. Vioglio, P.C.; Chierotti, M.R.; Gobetto, R. Pharmaceutical aspects of salt and cocrystal forms of APIS and characterization challenges. *Adv. Drug Deliv. Rev.* **2017**, *117*, 86–110. [[CrossRef](#)]
11. Cruz-Cabeza, A. Acid–base crystalline complexes and the pKa rule. *CrystEngComm* **2012**, *14*, 6362–6365. [[CrossRef](#)]
12. Nagalapalli, R.; Bheem, S.Y. Synthesis, Crystal Structure, and Hirshfeld Surface Analysis of Ciprofloxacin-Salicylic Acid Molecular Salt. *J. Crystallogr.* **2014**, *2014*, 936174. [[CrossRef](#)]
13. Surov, A.O.; Vasilev, N.A.; Churakov, A.V.; Stroh, J.; Emmerling, F.; Perlovich, G.L. Solid Forms of Ciprofloxacin Salicylate: Polymorphism, Formation Pathways, and Thermodynamic Stability. *Cryst. Growth Des.* **2019**, *19*, 2979–2990. [[CrossRef](#)]
14. Macrae, C.F.; Sovago, I.; Cottrell, S.J.; Galek, P.T.A.; McCabe, P.; Pidcock, E.; Platings, M.; Shields, G.P.; Stevens, J.S.; Towler, M.; et al. Mercury 4.0: From visualization to analysis, design and prediction. *J. Appl. Cryst.* **2020**, *53 Pt 1*, 226–235. [[CrossRef](#)]
15. Dalhoff, A.; Schubert, S.; Vente, A. Pharmacodynamics of Finafloxacin, Ciprofloxacin, and Levofloxacin in Serum and Urine against TEM- and SHV-Type Extended-Spectrum- $\beta$ -Lactamase-Producing Enterobacteriaceae Isolates from Patients with Urinary Tract Infections. *Antimicrob. Agents Chemother.* **2017**, *61*, e02446-16. [[CrossRef](#)] [[PubMed](#)]
16. Yamashita, H.; Hirakura, Y.; Yuda, M.; Teramura, T.; Terada, K. Detection of Cocrystal Formation Based on Binary Phase Diagrams Using Thermal Analysis. *Pharm. Res.* **2013**, *30*, 70–80. [[CrossRef](#)]
17. Cherukuvada, S.; Row, T.N.G. Comprehending the Formation of Eutectics and Cocrystals in Terms of Design and Their Structural Interrelationships. *Cryst. Growth. Des.* **2014**, *14*, 4187–4198. [[CrossRef](#)]
18. Stoler, E.; Warner, J.C. Non-Covalent Derivatives: Cocrystals and Eutectics. *Molecules* **2015**, *20*, 14833–14848. [[CrossRef](#)]
19. Chadha, R.; Gupta, S.; Shukla, G. Crystal habit, characterization and pharmacological activity of various crystal forms of arteether. *Acta Pharm. B* **2011**, *1*, 129–135. [[CrossRef](#)]
20. Wermuth, C.; Stahl, P. *Handbook of Pharmaceutical Salts*, 2nd ed.; Verlag Helvetica Chimica Acta: Zurich, Switzerland, 2011.

21. Rychkov, D.A.; Arkhipov, S.G.; Boldyreva, E.V. Simple and efficient modifications of well-known techniques for reliable growth of high-quality crystals of small bioorganic molecules. *J. Appl. Crystallogr.* **2014**, *47*, 1435–1442. [[CrossRef](#)]
22. Rager, T.; Hilfiker, R. Cocrystal Formation from Solvent Mixtures. *Cryst. Growth. Des.* **2012**, *10*, 3237–3241. [[CrossRef](#)]
23. Pubchem: Ciprofloxacin. Available online: [Pubchem.ncbi.nlm.nih.gov/compound/Ciprofloxacin](http://Pubchem.ncbi.nlm.nih.gov/compound/Ciprofloxacin) (accessed on 20 November 2019).
24. Pubchem: Salicylic Acid. Available online: [Pubchem.ncbi.nlm.nih.gov/compound/Salicylic-acid](http://Pubchem.ncbi.nlm.nih.gov/compound/Salicylic-acid) (accessed on 20 November 2019).
25. Han, L.; Zhang, K.; Ishida, H.; Froimowicz, P. Study of the Effects of Intramolecular and Intermolecular Hydrogen-Bonding Systems on the Polymerization of Amide-Containing Benzoxazines. *Macromol. Chem. Phys.* **2017**, *218*, 1600562. [[CrossRef](#)]
26. Schkesinger, C.; Bolte, M.; Schmidt, M.U. Challenging structure determination from powder diffraction data: Two pharmaceutical salts and one cocrystal with  $Z' = 2$ . *Z. Krist.-Cryst. Mater.* **2018**, *234*, 257–268. [[CrossRef](#)]
27. Zheng, H.; Xiong, J.; Zhao, Z.; Qiao, J.; Xu, D.; Miao, M.; He, L.; Wu, X. Preparation of Progesterone Co-Crystals Based on Crystal Engineering Strategies. *Molecules* **2019**, *24*, 3936. [[CrossRef](#)] [[PubMed](#)]
28. Basavoju, S.; Boström, D.; Velaga, S. Pharmaceutical cocrystal and salts of norfloxacin. *Cryst. Growth Des.* **2006**, *6*, 2699–2708. [[CrossRef](#)]
29. Martinez-Alejo, J.M.; Dominguez-Chavez, J.G.; Rivera-Islas, J.; Herrera-Ruiz, D.; Hoepfl, H.; Morales-Rojas, H.; Senosiain, J.P. A Twist in Cocrystals of Salts: Changes in Packing and Chloride Coordination Lead to Opposite Trends in the Biopharmaceutical Performance of Fluoroquinolone Hydrochloride Cocrystals. *Cryst. Growth Des.* **2014**, *14*, 3078–3095. [[CrossRef](#)]
30. Trivedi, M.K.; Branton, A.; Trivedi, D.; Shettigar, H.; Bairwa, K.; Jana, S. Fourier transform infrared and ultraviolet-visible spectroscopic characterization of biofield treated salicylic acid and sparfloxacin. *Nat. Prod. Chem. Res.* **2015**, *3*, 1000186. [[CrossRef](#)]
31. Neugebauer, U.; Szeghalmi, A.; Schmitt, M.; Kiefer, W.; Popp, J.; Holzgrabe, U. Vibrational spectroscopic characterization of fluoroquinolones. *Spectrochim. Acta A* **2005**, *61*, 1505–1517. [[CrossRef](#)]
32. Zhang, Y.; Yang, Z.; Zhang, S.; Zhou, X. Synthesis, Crystal Structure, and Solubility Analysis of a Famotidine Cocrystal. *Crystals* **2019**, *9*, 360. [[CrossRef](#)]
33. An, H.; Choi, I.; Kim, I.W. Melting diagrams of adefovir dipivoxil and dicarboxylic acids: An approach to assess cocrystal compositions. *Crystals* **2019**, *9*, 70. [[CrossRef](#)]
34. Poppler, A.C.; Corlett, E.K.; Pearce, H.; Seymour, M.P.; Reid, M.; Montgomery, M.G.; Brown, S.P. Single-crystal X-ray diffraction and NMR crystallography of a 1:1 cocrystal of dithianon and pyrimethanil. *Acta Cryst.* **2017**, *73*, 149–156.
35. Aitipamula, S.; Vangala, V.R. X-Ray crystallography and its role in understanding the physicochemical properties of pharmaceutical cocrystals. *J. Indian Inst. Sci.* **2017**, *97*, 227–243. [[CrossRef](#)]
36. Mahapatra, S.; Venugopala, K.N.; Row, T.N.G. A Device to Crystallize Organic Solids: Structure of ciprofloxacin, midazolam, and ofloxacin as targets. *Crys. Growth Des.* **2010**, *10*, 1866–1870. [[CrossRef](#)]
37. Woinska, M.; Grabowsky, S.; Dominiak, P.M.; Wozniak, K.; Jayatilaka, D. Hydrogen atoms can be located accurately and precisely by x-ray crystallography. *Sci. Adv.* **2016**, *2*, e1600192. [[CrossRef](#)] [[PubMed](#)]
38. Saganowska, P.; Wesolowski, M. DSC as a screening tool for rapid co-crystal detection in binary mixtures of benzodiazepines with co-formers. *J. Therm. Anal. Calorim.* **2018**, *133*, 785–795. [[CrossRef](#)]
39. Khan, S.B.; Alamry, K.A.; Alyahyawi, N.A.; Asiri, A.M. Nanohybrid based on antibiotic encapsulated layered double hydroxide as a drug delivery system. *Appl. Biochem. Biotechnol.* **2014**, *175*, 1412–1428. [[CrossRef](#)] [[PubMed](#)]
40. Jiang, W.T.; Wang, C.J.; Li, Z. Intercalation of ciprofloxacin accompanied by dehydration in rectorite. *Appl. Clay Sci.* **2013**, *74*, 74–80. [[CrossRef](#)]
41. Badea, M.; Olar, R.; Marinescu, D.; Uivarosi, V.; Iacob, D. Thermal decomposition of some biologically active complexes of ruthenium (III) with quinolone derivatives. *J. Therm. Anal. Calorim.* **2009**, *97*, 735. [[CrossRef](#)]
42. Satisharan, I.; Dalvi, S.V. Engineering Cocrystals of Poorly Water-Soluble Drugs to Enhance Dissolution in Aqueous Medium. *Pharmaceutics* **2018**, *10*, E108. [[CrossRef](#)]
43. Emami, S.; Shadbad, M.S.; Adibkia, K.; Jalali, M.B. Recent advances in improving oral drug bioavailability by cocrystals. *Bioimpacts* **2018**, *8*, 305–320. [[CrossRef](#)]

44. Scherer, R.; Pereira, J.; Firme, J.; Lemos, M.; Lemos, M. Determination of Ciprofloxacin in Pharmaceutical Formulations Using HPLC Method with UV Detection. *Indian J. Pharm. Sci.* **2014**, *76*, 541.
45. Emami, J.; Rezazadeh, M. A simple and sensitive high-performance liquid chromatography method for determination of ciprofloxacin in bioavailability studies of conventional and gastroretentive prolonged-release formulations. *Adv. Biomed. Res.* **2016**, *5*, 163. [[PubMed](#)]
46. Naveed, S.; Waheed, N.; Simple, U.V. Spectrophotometric Assay of Ciprofloxacin. *Mintage J. Pharm. Med. Sci.* **2014**, *5*, 10–13.
47. Badel, D.A.P.; Rivas, B.L.; Urbano, B. Ultrafiltration membranes with three water-soluble polyelectrolyte copolymers to remove ciprofloxacin from aqueous systems. *Chem. Eng. J.* **2018**, *351*, 85–93.
48. Perez, H.A.; Butos, A.; Taranto, M.P. Effects of Lysozyme on the Activity of Ionic of Fluoroquinolone Species. *Molecules* **2018**, *23*, 741. [[CrossRef](#)]
49. Guo, H.B.; He, F.; Gu, B.; Liang, L. Time-Dependent Density Functional Theory Assessment of UV Absorption of Benzoic Acid Derivatives. *J. Phys. Chem. A* **2012**, *116*, 11870–11879. [[CrossRef](#)]
50. Ahmad, I.; Sheraz, M.A.; Ahmed, S.; Anwar, Z. Multicomponent spectrometric analysis of drugs and their preparations. In *Profiles of Drug Substances, Excipients and Related Methodology*; Brittain, H., Ed.; Elsevier: Amsterdam, The Netherlands, 2018; pp. 379–413.
51. Surov, A.O.; Voronin, A.P.; Drozd, K.V.; Churakov, A.V.; Roussel, P.; Perlovich, G.L. Diversity of crystal structures and physicochemical properties of ciprofloxacin and norfloxacin salts with fumaric acid. *CrystEngComm* **2018**, *6*, 755–767. [[CrossRef](#)]
52. Bavishi, D.D.; Borkhataria, C.H. Spring and parachute: How cocrystals enhance solubility. *Prog. Cryst. Growth Charact.* **2016**, *62*, 1–8. [[CrossRef](#)]
53. Healy, A.M.; Worku, Z.A.; Kumar, D.; Madi, A.M. Pharmaceutical solvates, hydrates and amorphous forms: A special emphasis on cocrystals. *Adv. Drug Deliv. Rev.* **2017**, *117*, 25–46. [[CrossRef](#)]
54. Bezerra, D.M.; Zapelini, I.W.; Franke, K.M.; Ribeiro, M.E.; Cardoso, D. Investigation of the structural order and stability of mesoporous silicas under a humid atmosphere. *Mater. Charact.* **2019**, *154*, 103–115. [[CrossRef](#)]
55. Nugrahani, I.; Ibrahim, S.; Mauludin, R.; Almira, M. Hydrate transformation study of fluoroquinolone antibiotics using Fourier transform infrared spectroscopy (FTIR). *Int. J. Pharm. Pharm. Sci.* **2015**, *7*, 246–252.
56. Nugrahani, I.; Min, S.S. Hydrate transformation of sodium sulfacetamide and neomycin sulphate. *Int. J. Pharm. Pharm. Sci.* **2015**, *7*, 409–415.
57. Scaramuzza, D.; Rauber, G.S.; Voinovich, D.; Hasa, D. Dehydration without heating: Use of polymer-assisted grinding for understanding the stability of hydrates in the presence of polymeric excipients. *Cryst. Growth Des.* **2018**, *18*, 5245–5253. [[CrossRef](#)]
58. Ranu, B.; Stolle, A. *Ball Milling Towards Green Synthesis: Applications, Projects, Challenges*; RSC: Cambridge, UK, 2014; pp. 167–175.

